

Received March 5, 2019, accepted March 28, 2019, date of publication April 1, 2019, date of current version April 15, 2019.

Digital Object Identifier 10.1109/ACCESS.2019.2908720

Wavelet Deep Neural Network for Stripe Noise Removal

JUNTAO GUAN¹, RUI LAI¹, AND AI XIONG²

¹Department of Microelectronics, Xidian University, Xi'an 710071, China

²School of Control Engineering, Chengdu University of Information Technology, Chengdu 610103, China

Corresponding author: Rui Lai (rlai@mail.xidian.edu.cn)

This work was supported in part by the Natural Science Foundation of China (NSFC) under Grant 61674120, Grant 61571338, Grant U1709218, and Grant 61672131, in part by the Fundamental Research Funds for the Central Universities of China under Grant JBG161113 and Grant 300102328110, and in part by the Key Research and Development Plan of Shaanxi Province under Grant 2017ZDCXL-GY-05-01.

ABSTRACT The stripe noise effects severely degrade the image quality in infrared imaging systems. The existing despeckling algorithms still struggle to balance noise suppression, detail preservation, and real-time performance, which retards their application in spectral imaging and signal processing field. To solve this problem, an innovative wavelet deep neural network from the perspective of transform domain is presented in this paper, which takes the intrinsic characteristics of stripe noise and complementary information between the coefficients of different wavelet sub-bands into full consideration to accurately estimate the noise with the lower computational load. In addition, a special directional regularizer is further defined to separate the scene details from stripe noise more thoroughly and recover the details more accurately. The extensive experiments on simulated and real data demonstrate that our proposed method outperforms several classical despeckling methods on both quantitative and qualitative assessments.

INDEX TERMS Neural networks, image denoising, infrared image sensors, wavelet transforms.

I. INTRODUCTION

Infrared images have been widely used in applications such as remote sensing, medical diagnosis, visual tracking and IoT sensing [1]–[4]. Due to the restricts of fabrication process, the photoelectric response of detectors for the same irradiance may not be fully consistent, which results in fixed-pattern stripe noise superimposed on the observation and seriously decreases the sensitivity of the infrared imaging systems [5]–[7]. Hence, it is critical to remove the stripe noise and preserve the structures of the real scene simultaneously. The stripe noise degradation model can be formulated as

$$y(i, j) = x(i, j) + n(i, j) \quad (1)$$

where $y(i, j)$, $x(i, j)$ and $n(i, j)$ respectively stand for the observation, the ideal response and the stripe noise of the (i, j) th detector.

In recent years, many single image despeckling methods have been proposed under various frameworks. In general, these methods can be divided into three categories: prior-based methods, statistics-based methods and deep

The associate editor coordinating the review of this manuscript and approving it for publication was Yu Zhang.

learning based methods [8], [9]. As for the prior-based methods, block-matching and 3D filtering (BM3D) [10], total variation (TV) [11], guided filter (GF) [12], non-local means (NLM) filter [13] and low rank regularization [14] method employ the prior knowledge of the natural image to pursue better despeckling results. However, these methods tend to eliminate the details and stripe noise indiscriminately, which leads to obvious blurring artifacts in the output images. Statistics-based methods, just like midway histogram equalization (MHE) method [15], introduce the redundant information between adjacent columns to ameliorate the stripe noise disturbing. But they only work well for slight stripe noise. At present, deep learning based methods are extensively studied in image processing applications, and demonstrate amazing improvement on performance. Motivated by the state-of-the-art performance of deep learning, Kuang *et al.* proposed a three-layer stripe noise removal convolution neural network (SNRCNN) that directly treats the despeckling task as image denoising and super resolution [16] and leaves its own characteristics out of account, just for this reason, it is hard to remove the stripe noise thoroughly and retain the high frequency textures perfectly. In order to conquer this limitation, He *et al.* proposed DLSNUC model with

enlarged receptive fields to seek better destriping results [17]. Xiao *et al.* combined the local and global information in CNN and proposed the so-called ICSRNN model to optimize the edges preserving performance [18]. However, it is still struggling to handle the strong stripe noise. In summary, the existing deep learning based destriping methods only extract the features in spatial domain but ignore the abundant information contained in time-frequency domain, which severely limits the accuracy of stripe noise removal algorithm.

In the last decades, transform domain based image processing methods have been widely investigated [19], [20]. On this basis, Huang *et al.* proposed a super-resolution convolutional neural network (CNN) model to predict the missing details in wavelet domain [21]. Kang *et al.* characterized features via contourlet transformation, which yields outstanding performance in CT image denoising [22]. Inspired by these methods, we proposed an innovative strip noise removal wavelet deep neural network (SNRWDNN) model which exploits the special features involved in wavelet domain and utilizes the complementary information between sub-bands to perfectly remove stripe noise and retain image details. The main ideas and contributions of the paper are summarized as follows:

1. Introduce a deep neural network to directly learn the stripe noise features involved in wavelet domain, which contributes to precisely and adaptively estimate the noise strength and distribution.
2. Propose a directional regularizer to avoid the model producing irregular stripe and separate the scene details from stripe noise more accurately.
3. Utilize the wavelet decomposition to transform the input image into a series of quarter-sized coefficients, which significantly improves the computational efficiency and the destriping performance simultaneously.

The rest of this paper is organized as follows. In section 2, we analyze the property of strip noise in wavelet domain. Then the detail implementation of the proposed SNRWDNN model is presented in Section 3. To corroborate the effectiveness of the proposed method, both simulation and real data based experiments are described and analyzed in Section 4. Finally, we conclude the paper in Section 5.

II. PROPERTY ANALYSIS OF STRIPE NOISE

In order to estimate the stripe noise of the infrared image previously, the key issue is to excavate the properties of the stripe components and depict them with a proper method. As mentioned in [23], the stripe noise has a significant directional property which conduces to separate the noise components and image details in the destriping process. Figure 1 shows the gradient of the stripe noise corrupted image in horizontal and vertical direction. From the results, we can find that the stripe noise shows dense response in horizontal gradient and seriously affects the image textures distributed along vertical direction. In contrast, the vertical gradient of the stripe component exhibits good smoothness without disturbing the image details. Based on the above analysis, it is feasible to

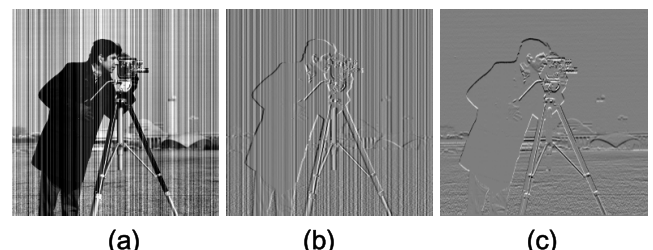


FIGURE 1. Directional property of stripe noise. (a) Stripe noise corrupted image; (b) Horizontal gradient of corrupted image; (c) Vertical gradient of corrupted image.

remove the stripe noise and retain the structures of the original image from the directional gradient perspective.

Haar Discrete Wavelet Transform (HDWT) [24] demonstrates the significant capability of extracting the high-frequency information in horizontal, vertical and diagonal directions as well as maintains the pattern structure in low-frequency sub-bands. In this paper, HDWT is employed to extract gradient information of the stripe noise and separate the scene details from stripe noise more thoroughly. Example results of HDWT are shown in Figure 2. It can be seen that the stripe noise shows an obvious response in approximation coefficients (cA) and horizontal coefficients (cH). In contrast, vertical coefficients (cV) and diagonal coefficients (cD) mainly depict the details in the scene. In summary, all the complementary information contained in different sub-bands will contribute to remove the stripe noise and preserve image details efficiently.

III. THE PROPOSED SNRWDNN MODEL

In this section, we will illustrate the detail structure of the proposed SNRWDNN model, and then further discuss the effectiveness of the special designed directional loss function for preserving textural details. Finally, the training strategy is described.

A. NETWORK ARCHITECTURE

The architecture of the proposed SNRWDNN is shown in Figure 3. Different from other existing deep learning based stripe noise removal methods, we treat the stripe noise removal as a transform coefficients prediction problem in wavelet domain. The SNRWDNN method consists of three steps: HDWT, wavelet coefficients prediction and Inverse Haar Discrete Wavelet Transform (IHDWT). Firstly, the HDWT is utilized to obtain the four sub-bands coefficients that reflect the intrinsic characteristics of stripe noise. Then these coefficients are concatenated as a single input tensor and fed into the wavelet coefficients prediction network to estimate the stripe component S , thereafter, the input tensor is skipingly connected with the estimated stripe component to perform noise cancellation and generate the destriped coefficients. It is worthy to note that the concatenation operation fuses the information in different sub-bands and keeps the consistency among them. Finally, the IHDWT is applied on the estimated coefficients to reconstruct the spatial domain

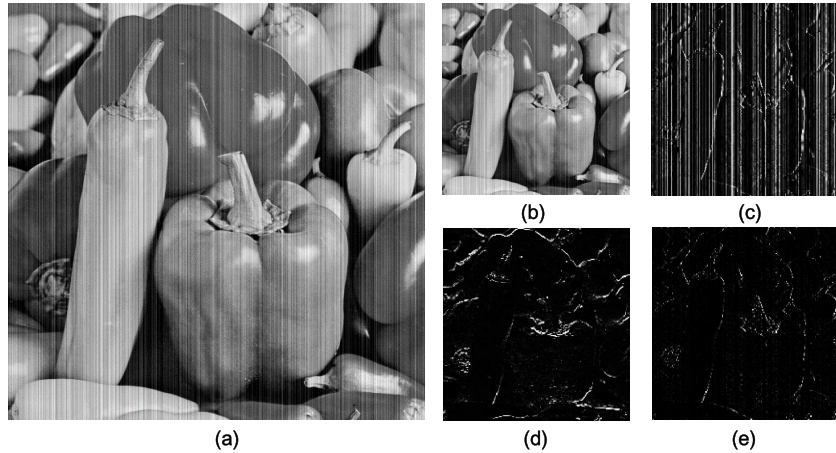
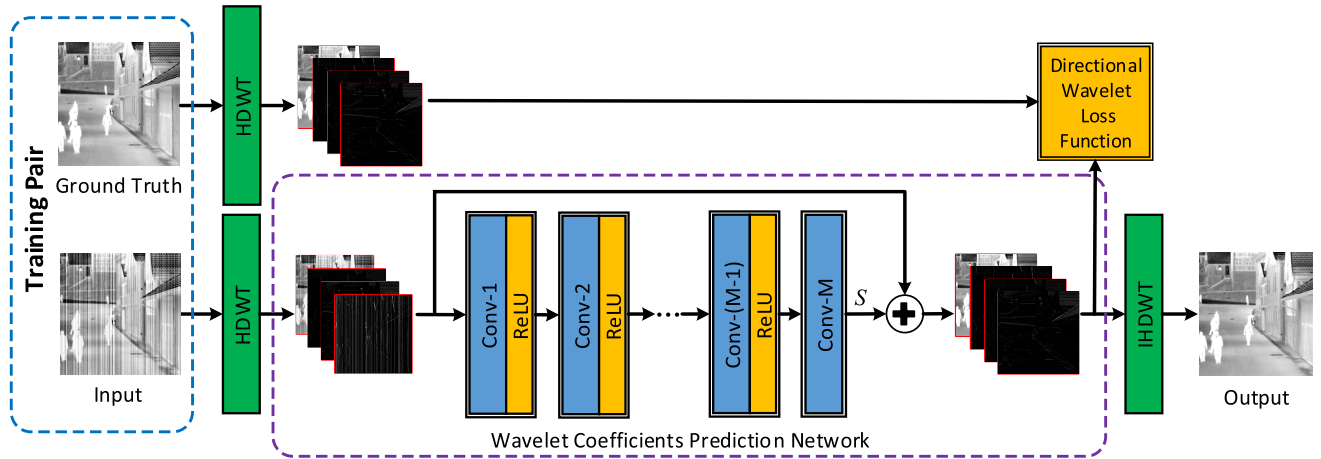


FIGURE 2. The HDWT of the stripe noise corrupted image (a) Noise corrupted image; (b) Approximation coefficients; (c) Horizontal coefficients; (d) Vertical coefficients; (e) Diagonal coefficients.



3

FIGURE 3. The network architecture of the proposed SNRWDNN method.

destriped results. With this tactic, our proposed network can utilize the directional characteristics of the stripe to suppress the noise with less detail loss.

The wavelet coefficients prediction network consists of M convolutional layers with residual connection, in which all the convolutional filters share the same size of 3×3 with a stride of 1. In addition, zero padding is adopted to make every feature map keep the same size with the input tensor. The kernel number of each convolutional layer is set to 64 except the last layer, who outputs 4-channel strip component. Moreover, the outputs of the former convolution layers are fed into Rectified Linear Unit (ReLU) activation function to perform nonlinear mapping. Since the input and output of the SNRWDNN are very similar, we adopt the residual learning for more stable, fast and precise training.

The down sampling operations in the wavelet decomposition effectively enlarge the receptive field, which is beneficial to the restoration of details in the scene [25].

Moreover, the wavelet decomposition significantly reduces the computational complexity.

B. DIRECTIONAL WAVELET LOSS FUNCTION

The optimization targets of recent deep learning based image processing methods generally focus on minimizing the Mean Square Error (MSE) loss function [26]. In this paper, we follow the literature [21], [25] and introduce a wavelet MSE loss to implement the stripe noise removal task in wavelet domain. The wavelet MSE loss is defined as

$$L_W = \|cA - \bar{c}A\|_2^2 + \|cV - \bar{c}V\|_2^2 + \|cH - \bar{c}H\|_2^2 + \|cD - \bar{c}D\|_2^2 \quad (2)$$

where $\|\cdot\|_2^2$ denotes the L2 norm, while cA , cV , cH and cD respectively stand for the approximation coefficients, horizon coefficients, vertical coefficients and diagonal coefficients of

the ground truth image, whose corresponding estimations are indicated by \bar{cA} , \bar{cV} , \bar{cH} , \bar{cD} .

From the local perspective, the intensity of pixels within a single stripe changes relatively in a narrow range, which means that the stripe possesses good smoothness in the along-stripe direction. In order to estimate the stripe noise more accurately, we describe the smoothness by minimizing the partial difference along the direction of estimated stripe component in stripe related sub-bands [27]. To do this, we construct the directional regularizer as

$$L_D = \|\nabla S_{cA}\|_2^2 + \|\nabla S_{cH}\|_2^2 \quad (3)$$

where ∇ denotes the partial difference operator along stripe direction. S_{cA} and S_{cH} stands for the stripe component of cA and cH sub-bands, respectively.

Finally, the proposed directional wavelet loss function is defined as

$$\text{Loss} = L_W + \lambda \cdot L_D \quad (4)$$

where λ is a balance scalar to control the weight of the directional loss.

C. TRAINING STRATEGY

The publicly available dataset BSDS500 [28] is used to train the proposed SNRWDNN model. We employ the data augmentation with rotation and flip to generate 230,000 patches of 64×64 sized images, and then corrupt them using stripe noise with mean 0 and standard deviation from 0 to 0.25 according to Equation (1) [29]. In addition, the test dataset called Set12 [30] is adopted to evaluate the performance of different destriping methods. It is worthy of note that Set12 is a widely used benchmark for most image denoising and restoration works and not included in the training dataset.

In the training phase, Keras package [31] was employed to implement the proposed SNRWDNN model. The depth M of SNRWDNN is set to 10 and the balance scalar λ in the loss function is set to 0.5. The adaptive moment estimation (ADAM) optimization method [32] is adopted to optimize our network. In addition, the batch size and weight decay is set to 128 and 1×10^{-6} , respectively. The learning rate is initially set to 0.001 and then decreased by the factor of 0.5 every 10 epochs. The maximum number of training epochs is set to 50. The training phase only takes about 2 hours on single NVidia 1080Ti GPU.

IV. EXPERIMENTS

In this section, we will firstly analyze the relationship between the SNRWDNN structure and the destriping performance promotion. Subsequently, the effectiveness of the proposed SNRWDNN method will be further verified and compared with the classical destriping methods on both of the artificially corrupted data and real noisy data.

A. ANALYSIS OF THE NETWORK STRUCTURE

In order to determine the optimal structure for the proposed SNRWDNN model, the residual learning strategy, directional regularizer function and configuration of the input tensor will be meticulously discussed in this section.

1) EFFECTIVENESS OF RESIDUAL LEARNING

To demonstrate the effectiveness of the residual learning strategy, we remove the residual connections [33] from the proposed SNRWDNN model and build a modified version with a structure similar to the SNRCNN model. Following that, the SNRWDNN models with and without residual connections are both employed to perform the same stripe noise removal task on the same test dataset.

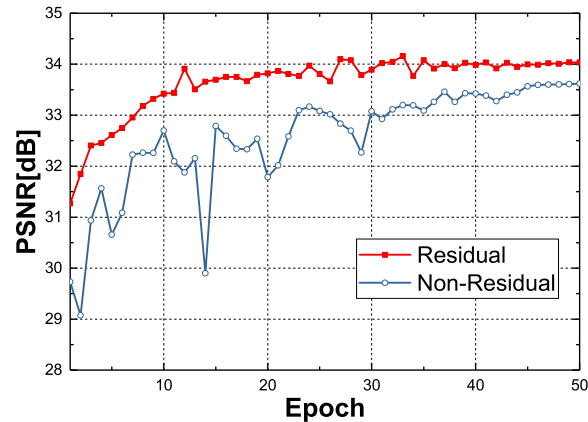


FIGURE 4. PSNR curves of the proposed SNRWDNN model with and without residual connections.

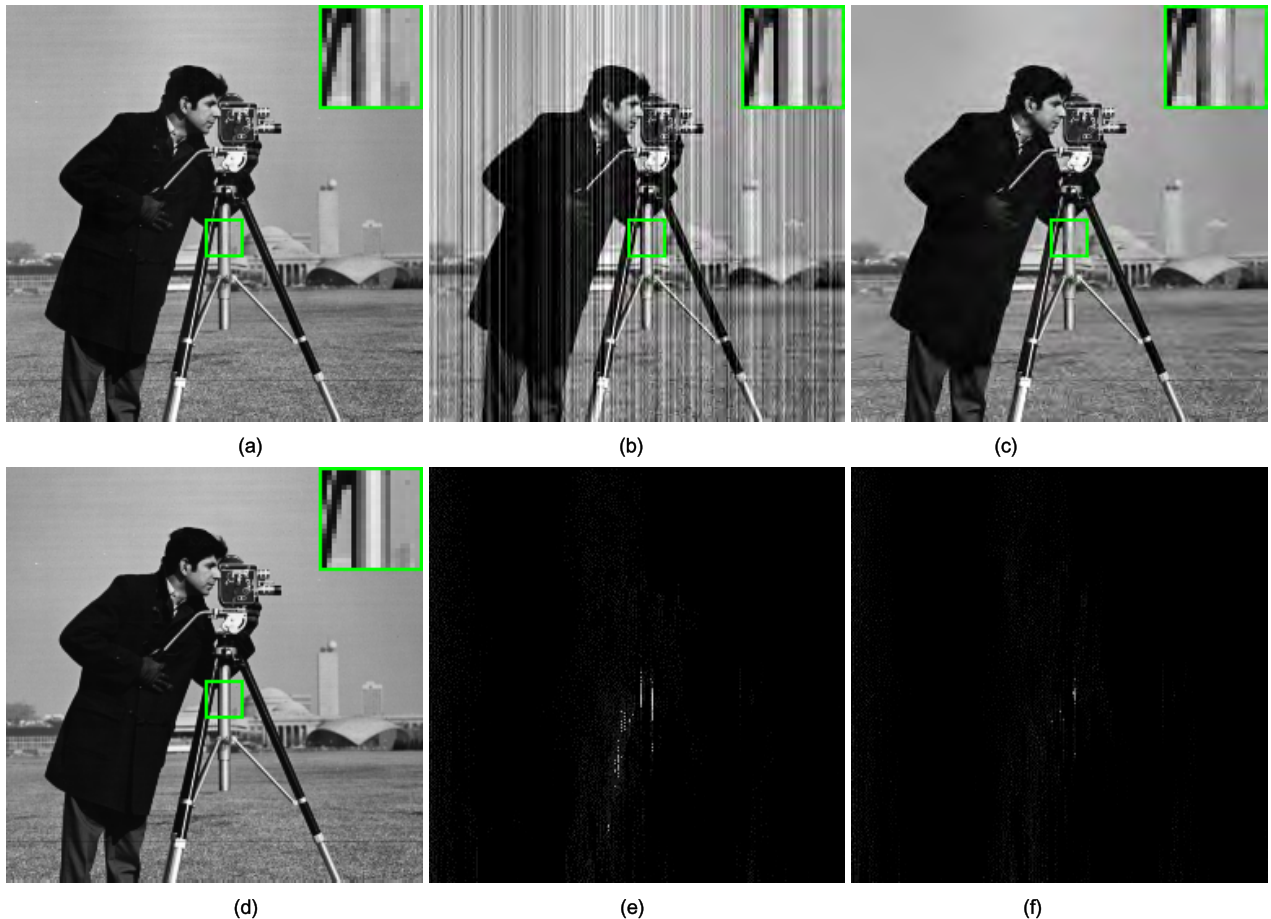
The learning curves for each model regarding the PSNR on the benchmark are shown in Figure 4. It can be seen clearly that the performance of non-residual architecture fluctuates violently and converges more slowly. In contrast, the SNRWDNN model with residual connections converges more stably and swiftly. Moreover, the residual architecture achieves about 0.4dB higher PSNR over the non-residual architecture in the whole training process. In short, the residual learning strategy is powerful and effective for achieving more stable convergence and remarkable performance improvement.

2) EFFECTIVENESS OF DIRECTIONAL REGULARIZER

In order to verify the effectiveness of the proposed directional regularizer, we respectively train two versions of SNRWDNN models by using the loss function with and without directional regularizer. The experiment is carried on several images corrupted by stripe noise with standard deviation 0.05 and 0.1, respectively. The PSNR results are summarized in Table 1, in which the best results for each noise level are highlighted in bold. It can be seen that the SNRWDNN model trained with loss function involving directional regularizer shows a significant higher PSNR in most cases, while the negligible PSNR reduction occurs only once in each noise

TABLE 1. PSNR results of various loss function on test images.

Loss Function \ Images	Cam.Man	Pepper	Starfish	Butterfly	Airplane	Barbara	Average
Noise level = 0.05							
With Directional Regularizer	35.67	33.02	34.66	34.03	31.80	34.52	33.95
Without Directional Regularizer	34.86	32.56	34.03	34.07	31.33	34.18	33.51
Noise level = 0.1							
With Directional Regularizer	31.27	28.69	30.20	29.48	28.30	30.52	29.74
Without Directional Regularizer	30.63	28.01	30.15	29.31	28.07	30.55	29.46

**FIGURE 5.** Destriping results of the proposed SNRWDNN model with and without directional regularizer. (a) Original image; (b) Corrupted image; (c) Destriping results without directional regularizer; (d) Destriping results with directional regularizer; (e) Difference image between (c) and (a); (f) Difference image between (d) and (a).

level. The reason lies in that the directional regularizer conducts to estimate the stripe noise more precisely and avoids removing scene details resemble the stripe noise.

Figure 5 illustrates the visual effect comparison for the destriping results of abovementioned two loss functions. As can be seen from Figure 5 (c) and (d), both of the loss functions can efficiently remove the stripe noise. By observing more carefully, we can find the enlargement of the square region in Figure 5 (d) shows more sharp and clear vertical edge when compared with Figure 5 (c), which indicates the

directional regularizer is beneficial to preserve the edges along the direction of stripe by separating the scene details from stripe noise more accurately. From the difference image between directional regularizer acting destriping results and original image shown in Figure 5 (f), we can observe few signs of residual. In contrast, the loss function without directional regularizer results in the difference image with obvious residual shown in Figure 5 (e). This simulation further proves the effectiveness of the proposed directional regularizer for detail preserving.

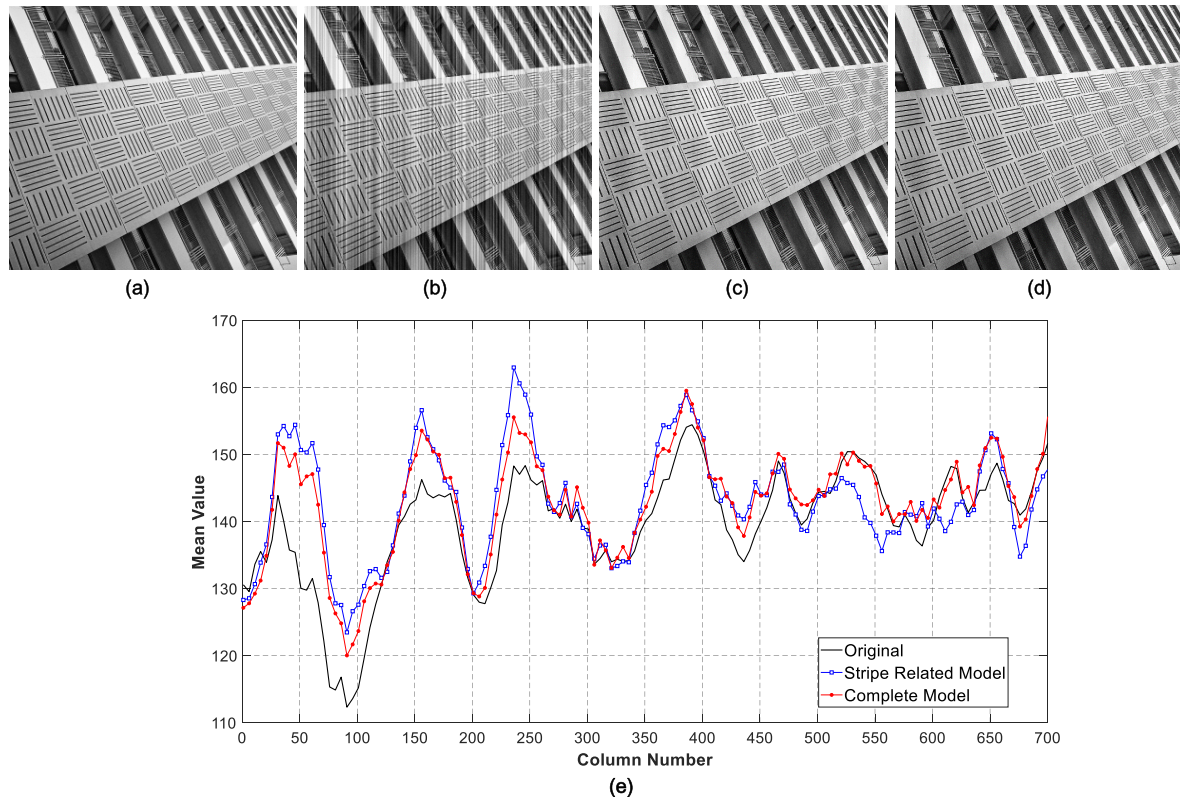


FIGURE 6. Despeckling results of simulated stripe noise. (a) Original image; (b) Corrupted image; (c) Result of stripe related model; (d) Result of complete model; (e) Mean value comparison between the despeckling results estimated by stripe related model and complete model.

3) ANALYSIS OF COMPLEMENTARITY BETWEEN WAVELET SUB-BANDS

In order to evaluate the influence of the complementary information between the different wavelet sub-bands on despeckling results, we train the proposed SNRWDNN model only using the stripe noise related sub-bands (cA and cH) and call it as stripe related model, and then employ all of the coefficients (cA , cV , cH and cD) to train the complete model. The despeckling results of two models were shown in Figure 6. As can be seen, there exist minor difference for despeckling results between these two models in visual effects. In order to show the difference more clearly, we show the mean cross-track curves in Figure 6(e). The horizontal axis denotes the column number and the vertical axis indicates the mean value of each column of the image. By comparison, we can find that the stripe related model fails to track the curve of original sample, which means the complete model is more adept in precisely removing the stripe noise as well as preserving details by employing the complementary information between wavelet sub-bands.

B. COMPARISON WITH CLASSICAL METHODS

In this section, we illustrate the quantitative and qualitative performance evaluation for the proposed SNRWDNN model. In the following experiments, two objective metrics of peak signal-to-noise ratio (PSNR) and structural similarity index (SSIM) [34] are employed to assess the despeckling

performance by comparing the proposed method with the following seven classical methods as:

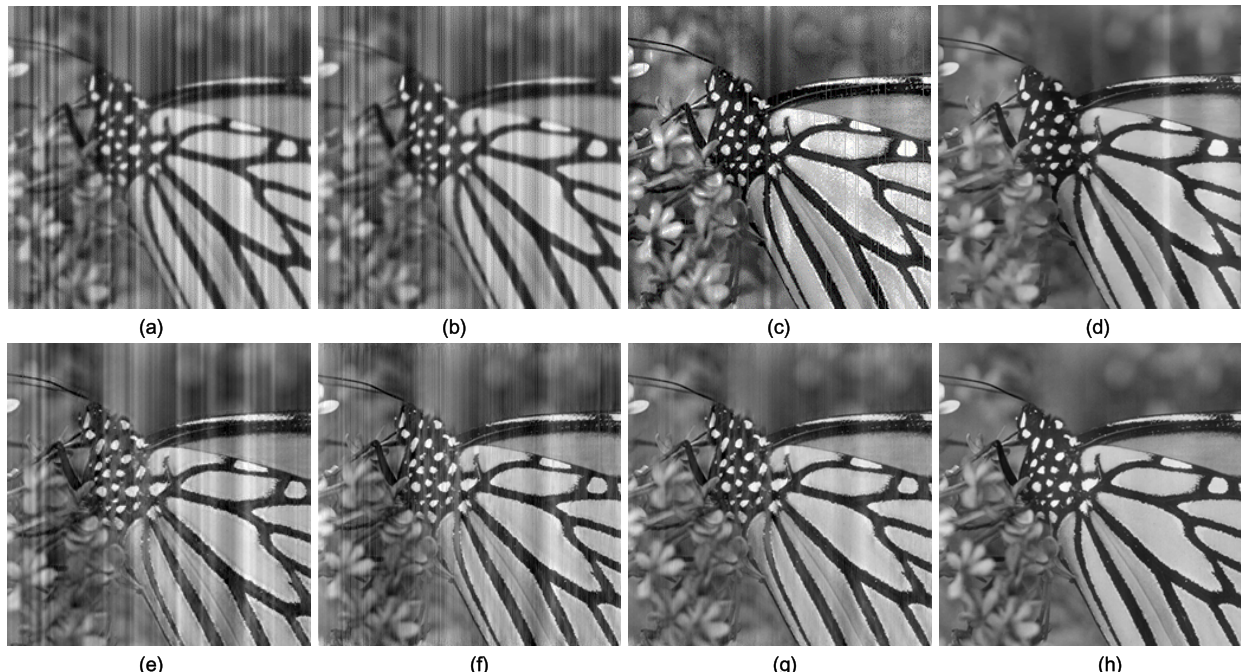
- 1) Guided Filter (GF) method [12]
- 2) Non-local Mean Filter (NLM) method [13]
- 3) Midway Histogram Equalization (MHE) method [15]
- 4) Low-Rank Single-Image Decomposition (LRSID) model [14]
- 5) Stripe Noise Removal Convolution Neural Network (SNRCNN) method [16]
- 6) Deep Learning-based Stripe Nonuniformity Correction (DLSNUC) method [17]
- 7) Infrared image Stripe Noise Removal Network (ICSRN) method [18]

1) SIMULATION WITH ARTIFICIALLY CORRUPTED DATA

In the simulation, the test dataset Set12 is adopted to evaluate the performance of different despeckling methods. The mean PSNR and SSIM results of various methods are shown in Table 2 and the best results for each noise level are highlighted in bold. As can be seen, the deep learning based SNRCNN, DLSNUC and ICSRNN provide more notable promotion in PSNR and SSIM than GF, NLM and MHE. However, LRSID achieves better results than SNRCNN, DLSNUC and ICSRNN method due to the effective low-rank constraints. Significantly, our SNRWDNN model yields more remarkable improvement on both of PSNR and SSIM upon the recent SNRCNN, DLSNUC and ICSRNN method.

TABLE 2. Mean PSNR/SSIM results of various desstriping methods on set12.

Noise Level	Corrupted Image	Desstriping Results							
		GF	NLM	MHE	LRSID	SNRCNN	DLSNUC	ICSRN	SNRDWNN
0.06	25.08/0.6023	27.36/0.8029	26.97/0.7782	27.86/0.8792	30.63/0.9426	28.13/0.9444	28.46/0.9502	28.73/0.9579	33.18/0.9878
0.1	20.74/0.4256	24.91/0.7043	24.48/0.6597	24.91/0.8122	29.42/0.9377	26.44/0.9286	26.56/0.9398	26.98/0.9466	30.07/0.9818
0.14	17.94/0.3211	23.05/0.6287	22.86/0.5725	22.45/0.7467	27.90/0.9273	24.79/0.9064	25.01/0.9179	25.26/0.9307	28.01/0.9761
0.18	15.92/0.2535	21.68/0.5874	21.37/0.5028	20.46/0.6804	26.23/0.9077	23.28/0.8770	23.45/0.8976	23.72/0.9108	26.43/0.9702
0.22	14.37/0.2066	20.71/0.5547	20.24/0.4453	18.77/0.6129	24.51/0.8735	21.93/0.8423	22.13/0.8729	22.36/0.8873	25.12/0.9638

**FIGURE 7.** Desstriping results of the image “Butterfly” with noise level 0.14. (a) Results of GF; (b) Result of NLM; (c) Result of MHE; (d) Result of LRSID; (e) Result of SNRCNN; (f) Result of DLSNUC; (g) Result of ICSRN; (h) Result of the proposed SNRDWNN.

Moreover, the SSIM decreases gently with the noise strength sharply growing. The abovementioned outstanding results are benefited from the abundant complementary information excavated by deep learning from wavelet sub-bands.

Figure 7 illustrates the visual effects of different desstriping methods. It can be seen that GF and NLM smooth the image without making a distinction between noise and details. These mechanisms inevitably damage the image details and lead to heavy noise residue. The MHE method removes the stripe noise efficiently, but it suffers from obvious brightness distortion near image edges. Although the LRSID method preserves the image details and removes most of the stripe noise efficiently, it fails to address the strong stripe noise. The deep learning based SNRCNN, DLSNUC and ICSRN methods preserve most details but still struggle to suppress the stripe noise thoroughly. In contrast, the proposed SNRDWNN model not only removes almost all the stripe noise but also preserves the sharp details and yields visual pleasant results.

In order to further embody the stripe noise removal ability of the proposed method, we show the desstriping results of various methods on different noise level in Figure 8. As can be seen, along with the increase of noise level, the SNRCNN, DLSNUC and ICSRN produce a noticeable noise residual and structural detail damage. In contrast, the desstriping result of the SNRDWNN is more close to the original image in human perception, which implies that the proposed method could effectively distinguish the noise components and original structure in the desstriping process. It is worth noting that the noise level 0.38 is not included in the training phase, the results further prove the powerful desstriping ability of the proposed SNRDWNN model.

2) VALIDATIONS ON REAL INFRARED IMAGES

In order to validate the effectiveness of the proposed method in practical application, we assess the performance of the SNRDWNN model on real noisy image captured by

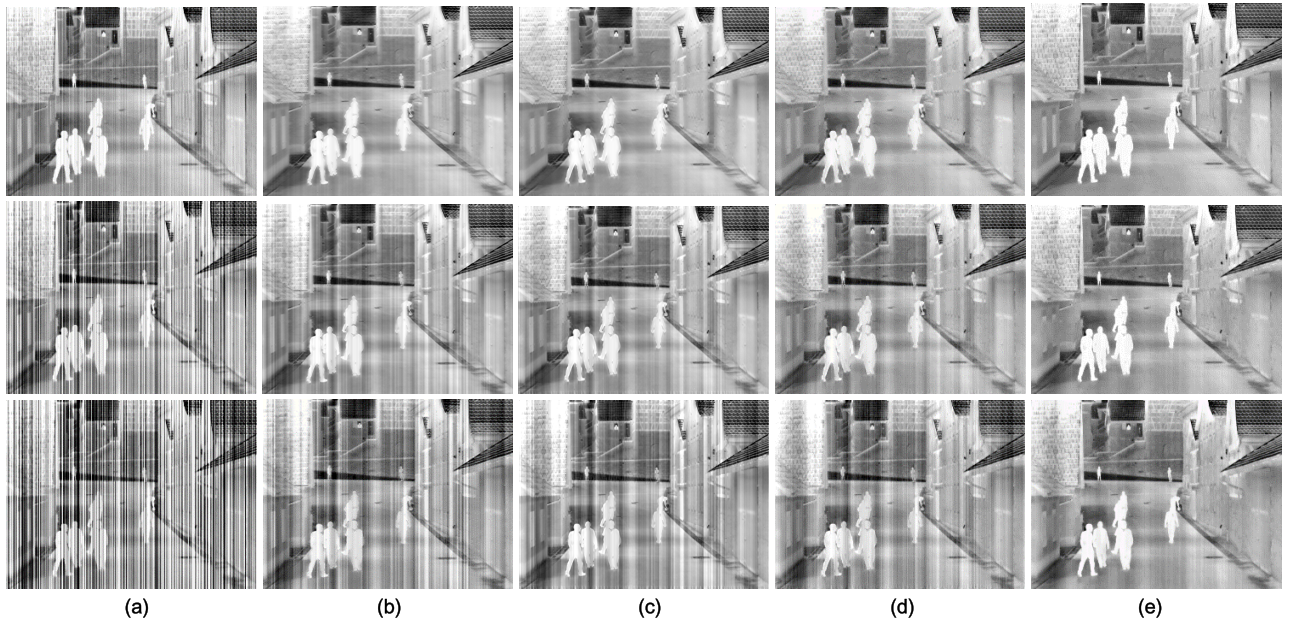


FIGURE 8. Destriping results of different methods on infrared image "Street" with noise level 0.06, 0.22 and 0.38 from top to bottom, respectively. (a) Corrupted image. (b) SNRCNN. (c) DLSNUC. (d) ICSRN. (e) SNRWDNN.

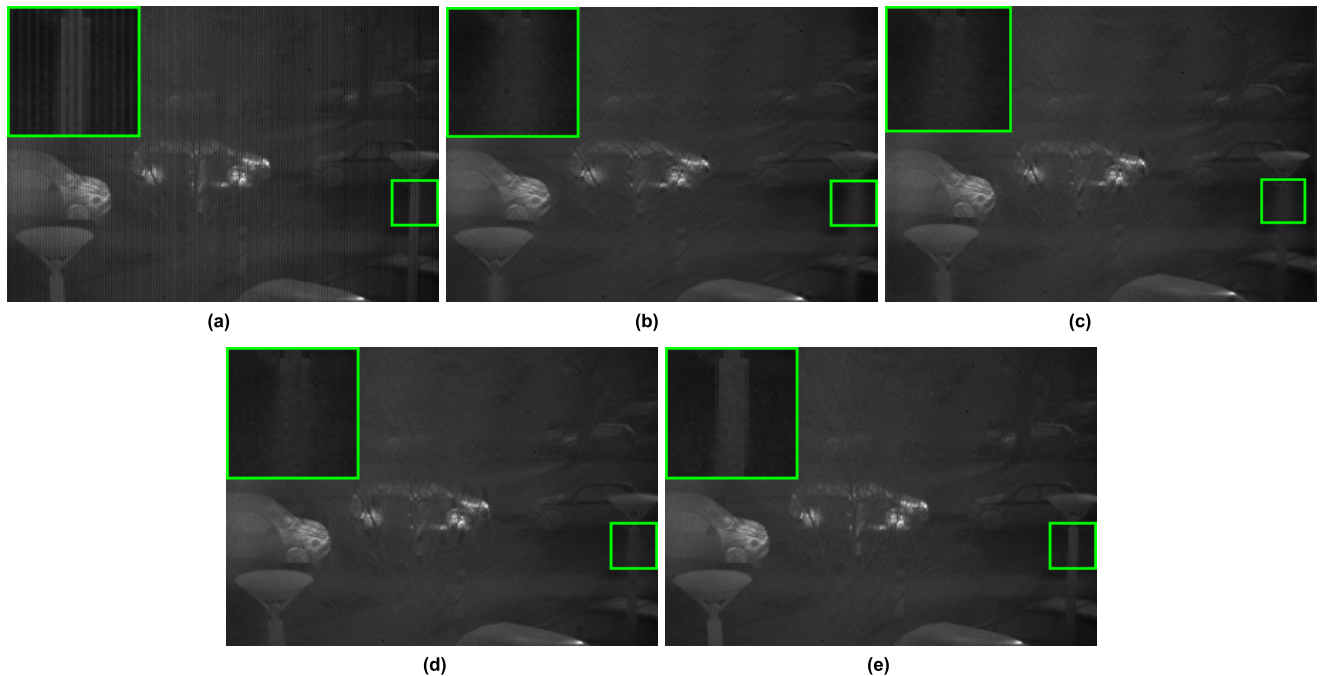


FIGURE 9. Destriping results of various methods for the infrared image of streetscape. (a) Raw infrared image (b) Result of SNRCNN (c) Result of DLSNUC (d) Result of ICSRN (e) Results of the proposed SNRWDNN.

infrared cameras. The visual effects of various destriping methods are shown in Figure 9. In view of the prior based methods and MHE method are hardly to achieve balanced and satisfied results in destriping task, we only implement the comparison of the deep learning based methods in this experiment. The destriping results of SNRCNN, DLSNUC, ICSRN and SNRWDNN are shown in Figure 9 (b)-(e), respectively. It is clear that SNRCNN, DLSNUC and ICSRN

can effectively suppress the thin and dense stripe noise. However, the SNRCNN method generates very notable over smooth results in vertical textures area, which is due to the weak expression ability of the too shallow network. The DLSNUC and ICSRN avoid serious over smooth artifacts by enlarging the receptive field and increasing the depth of the network, but even then, they still damage the image details visibly. In contrast, the proposed SNRWDNN method

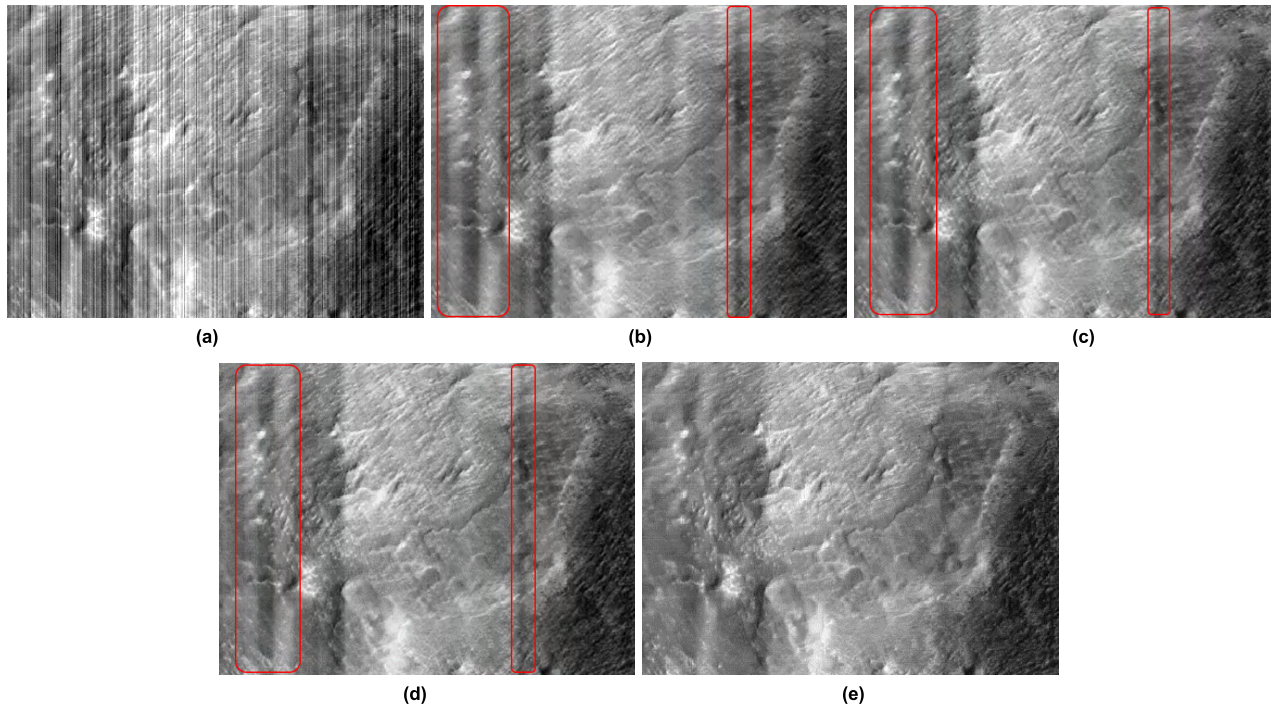


FIGURE 10. Despeckling results of various methods for the infrared image of Mars surface. (a) Raw infrared image (b) Result of SNRCNN (c) Result of DLSNUC (d) Result of ICSRN (e) Result of the proposed SNRWDNN.

learns the features in wavelet domain and fully considers the directional property of stripe noise, which leads to the best restoration quality.

In addition, we further implement visual effect comparison on Mars Orbiter satellite collecting infrared image corrupted by strong stripe noise [35]. The results of various despeckling methods are shown in Figure 10. As can be seen, the SNRCNN, DLSNUC and ICSRN still suffer from the noise residue artifacts in varying extent, which are marked out with red box. In contrast, the proposed SNRWDNN method more thoroughly suppresses the stripe noise without destroying the intrinsic structure of the image, which yields more sharp and clear details of the Mars surface. In conclusion, the proposed SNRWDNN model also exhibits the most prominent performance in real-world scenarios.

3) RUNTIME COMPARISON

Deep learning based methods generally consume a large amount of computation to exchange for outstanding performance, which limits the popularization and application of these methods in real-time systems. To completely illustrate the running speed of the proposed method, we perform the simulated experiment on images with various sizes and list the runtime in Table 3. It can be seen that the SNRCNN achieves the best result which is resulted from its shallow network architecture. Although the DLSNUC method employs pooling operation to reduce the computational load, it is still slower than the proposed SNRWDNN method. The ICSRN is the most time-consuming method for the huge network parameters. In contrast, the proposed SNRWDNN

TABLE 3. Runtime (ms) of various despeckling methods on different image.

Image Size	SNRCNN	DLSNUC	ICSRN	SNRWDNN
320×220	2.99	4.99	14.95	3.99
256×256	3.98	5.41	15.96	4.98
384×288	4.99	6.99	22.93	5.98
512×512	10.09	15.99	49.98	10.96

method achieves a high processing speed close to the shallow SNRCNN model. The reason lies in that SNRWDNN method performs the time-consuming convolutional operation in parallel for multi-channel quarter-sized coefficients which significantly reduce the computational complexity.

In summary, compared with traditional GF, NLM, MHE and LRSID method, the proposed SNRWDNN consumes huge hardware resources to gain amazing performance promotion. On the other hand, the proposed method has more promising time efficiency and higher performance than the deep learning based SNRCNN, DLSNUC and ICSRN method, which makes it closer to the realization of real-time processing on terminal equipment.

V. CONCLUSIONS

In this paper, we proposed an innovative SNRWDNN model for stripe noise removal. Different from the existing despeckling methods, the SNRWDNN method utilizes the HDWT to depict the directional property of stripe components and employs the complementary information between different sub-bands to predict the noise strength and distribution.

Moreover, the special designed directional regularizer function is proposed to separate the scene details from stripe noise and prevent irregular stripe in estimation. Experimental results indicate that our method yields outstanding desstriping precision and achieves amazing visual effect for human vision perception. We contend that wavelets analysis provides a time-frequency representation reflecting the intrinsic characteristics of images more comprehensively and simplifies the mapping to be learned. In view of this, it is promising to embed the framework of proposed wavelet deep neural network (WDNN) as the pre-procedure to promote the performance of image classification [36] and signal processing [37]–[39].

In spite of the superior performance achieved by the proposed method, it still suffers from the drawbacks of relatively large computation requirement and detail loss under strong noise level.

In future work, we will optimize our model to reduce the computational load by employing the recent proposed depth wise separable convolution [40] and apply our approach to hardware implementation for better real-time performance with smaller power consumption. In addition, the more advanced wavelet functions, such as shearlets [41], will be introduced into our desstriping model to excavate structural information in more depth and separate the stripe noise and details more thoroughly.

REFERENCES

- [1] A. Jara *et al.*, “Joint de-blurring and nonuniformity correction method for infrared microscopy imaging,” *Infr. Phys. Technol.*, vol. 90, pp. 199–206, May 2018.
- [2] Y. Cao and Y. Li, “Strip non-uniformity correction in uncooled long-wave infrared focal plane array based on noise source characterization,” *Opt. Commun.*, vol. 339, pp. 236–242, Mar. 2015.
- [3] Y. Huang, C. He, H. Fang, and X. Wang, “Iteratively reweighted unidirectional variational model for stripe non-uniformity correction,” *Infr. Phys. Technol.*, vol. 75, pp. 107–116, Mar. 2016.
- [4] C. Chen, X. Liu, H.-H. Chen, M. Li, and L. Zhao, “A rear-end collision risk evaluation and control scheme using a Bayesian network model,” *IEEE Trans. Intell. Transp. Syst.*, vol. 20, no. 1, pp. 264–284, Jan. 2019.
- [5] R. Lai, G. Yue, and G. Zhang, “Total variation based neural network regression for nonuniformity correction of infrared images,” *Symmetry*, vol. 10, no. 5, p. 157, 2018.
- [6] R. Lai, J. Guan, Y. Yang, and A. Xiong, “Spatiotemporal adaptive nonuniformity correction based on BTV regularization,” *IEEE Access*, vol. 7, pp. 753–762, 2019.
- [7] K. Liang, C. Yang, L. Peng, and B. Zhou, “Nonuniformity correction based on focal plane array temperature in uncooled long-wave infrared cameras without a shutter,” *Appl. Opt.*, vol. 56, no. 4, pp. 884–889, 2017.
- [8] X. Jian, R. Lu, Q. Guo, and G.-P. Wang, “Single image non-uniformity correction using compressive sensing,” *Infr. Phys. Technol.*, vol. 76, pp. 360–364, May 2016.
- [9] S. Rong, H. Zhou, D. Zhao, K. Cheng, K. Qian, and H. Qin, “Infrared fix pattern noise reduction method based on shearlet transform,” *Infr. Phys. Technol.*, vol. 91, pp. 243–249, Jun. 2018.
- [10] K. Dabov, A. Foi, and K. Egiazarian, “Video denoising by sparse 3D transform-domain collaborative filtering,” in *Proc. Eur. Signal Process. Conf.*, Poznan, Poland, Sep. 2007, pp. 145–149.
- [11] L. I. Rudin, S. Osher, and E. Fatemi, “Nonlinear total variation based noise removal algorithms,” *Phys. D, Nonlinear Phenomena*, vol. 60, nos. 1–4, pp. 259–268, 1992.
- [12] K. He, J. Sun, and X. Tang, “Guided image filtering,” *IEEE Trans. Pattern Anal. Mach. Intell.*, vol. 35, no. 6, pp. 1397–1409, Jun. 2013.
- [13] H. Li and C. Y. Suen, “A novel non-local means image denoising method based on grey theory,” *Pattern Recognit.*, vol. 49, pp. 237–248, Jan. 2016.
- [14] Y. Chang, L. Yan, T. Wu, and S. Zhong, “Remote sensing image stripe noise removal: From image decomposition perspective,” *IEEE Trans. Geosci. Remote Sens.*, vol. 54, no. 12, pp. 7018–7031, Dec. 2016.
- [15] Y. Tendero, J. Gilles, S. Landeau, and J. M. Morel, “Efficient single image non-uniformity correction algorithm,” *Proc. SPIE*, vol. 7834, Oct. 2010, Art. no. 78340E.
- [16] X. Kuang, X. Sui, Q. Chen, and G. Gu, “Single infrared image stripe noise removal using deep convolutional networks,” *IEEE Photon. J.*, vol. 9, no. 4, Aug. 2017, Art. no. 3900913.
- [17] Z. He, Y. Cao, Y. Dong, J. Yang, Y. Cao, and C.-L. Tisse, “Single-image-based nonuniformity correction of uncooled long-wave infrared detectors: A deep-learning approach,” *Appl. Opt.*, vol. 57, no. 18, pp. D155–D164, 2018.
- [18] P. Xiao, Y. Guo, and P. Zhuang, “Removing stripe noise from infrared cloud images via deep convolutional networks,” *IEEE Photon. J.*, vol. 10, no. 4, Aug. 2018, Art. no. 7801114.
- [19] S. G. Chang, B. Yu, and M. Vetterli, “Adaptive wavelet thresholding for image denoising and compression,” *IEEE Trans. Image Process.*, vol. 9, no. 9, pp. 1532–1546, Sep. 2000.
- [20] A. L. da Cunha, J. Zhou, and M. N. Do, “The nonsubsampled contourlet transform: Theory, design, and applications,” *IEEE Trans. Image Process.*, vol. 15, no. 10, pp. 3089–3101, Oct. 2006.
- [21] H. Huang, R. He, Z. Sun, and T. Tan, “Wavelet-SRNet: A wavelet-based CNN for multi-scale face super resolution,” in *Proc. IEEE Conf. CVPR*, Honolulu, HI, USA, Oct. 2017, pp. 1689–1697.
- [22] E. Kang, J. Min, and J. C. Ye, “A deep convolutional neural network using directional wavelets for low-dose X-ray CT reconstruction,” *Med. Phys.*, vol. 44, no. 10, pp. e360–e375, 2017.
- [23] Y. Chen, T.-Z. Huang, L.-J. Deng, X.-L. Zhao, and M. Wang, “Group sparsity based regularization model for remote sensing image stripe noise removal,” *Neurocomputing*, vol. 267, pp. 95–106, Dec. 2017.
- [24] B. L. Lai and L. W. Chang, “Adaptive data hiding for images based on harr discrete wavelet transform,” in *Advances in Image and Video Technology* (Lecture Notes in Computer Science), vol. 4319, Berlin, Germany: Springer, 2006, pp. 1085–1093.
- [25] H. Chen, X. He, L. Qing, S. Xiong, and T. Q. Nguyen, “DPW-SDNet: Dual pixel-wavelet domain deep CNNs for soft decoding of JPEG-compressed images,” presented at the IEEE Conf. CVPR, Salt Lake City, UT, USA, 2018.
- [26] C. Ledig *et al.*, “Photo-realistic single image super-resolution using a generative adversarial network,” in *Proc. IEEE Conf. CVPR*, Honolulu, HI, USA, Jul. 2017, pp. 105–114.
- [27] X. Liu, X. Lu, H. Shen, Q. Yuan, Y. Jiao, and L. Zhang, “Stripe noise separation and removal in remote sensing images by consideration of the global sparsity and local variational properties,” *IEEE Trans. Geosci. Remote Sens.*, vol. 54, no. 5, pp. 3049–3060, May 2016.
- [28] W. Luo, J. Li, W. Xu, and J. Yang, “Learning sparse features in convolutional neural networks for image classification,” in *Proc. Int. Conf. Intell. Sci. Big Data Eng.*, Suzhou, China, 2015, pp. 29–38.
- [29] K. Simonyan and A. Zisserman. (2014). “Very deep convolutional networks for large-scale image recognition.” [Online]. Available: <https://arxiv.org/abs/1409.1556>
- [30] K. Zhang, W. Zuo, Y. Chen, D. Meng, and L. Zhang, “Beyond a Gaussian denoiser: Residual learning of deep CNN for image denoising,” *IEEE Trans. Image Process.*, vol. 26, no. 7, pp. 3142–3155, Jul. 2017.
- [31] D. Graziotin and P. Abrahamsson, “A Web-based modeling tool for the SEMAT essence theory of software engineering,” *J. Open Res. Softw.*, to be published. doi: [10.5334/jors.ad](https://doi.org/10.5334/jors.ad).
- [32] D. P. Kingma and J. Ba. (2014). “Adam: A method for stochastic optimization.” [Online]. Available: <https://arxiv.org/abs/1412.6980>
- [33] J. Kim, J. K. Lee, and K. M. Lee, “Accurate image super-resolution using very deep convolutional networks,” in *Proc. IEEE Conf. CVPR*, Las Vegas, NV, USA, Jun. 2016, pp. 1646–1654.
- [34] Z. Wang, A. C. Bovik, H. R. Sheikh, and E. P. Simoncelli, “Image quality assessment: From error visibility to structural similarity,” *IEEE Trans. Image Process.*, vol. 13, no. 4, pp. 600–612, Apr. 2004.
- [35] Y. Cao, M. Y. Yang, and C.-L. Tisse, “Effective strip noise removal for low-textured infrared images based on 1-D guided filtering,” *IEEE Trans. Circuits Syst. Video Technol.*, vol. 26, no. 12, pp. 2176–2188, Dec. 2016.
- [36] N. Liu, L. Wan, Y. Zhang, T. Zhou, H. Huo, and T. Fang, “Exploiting convolutional neural networks with deeply local description for remote sensing image classification,” *IEEE Access*, vol. 6, pp. 11215–11228, 2018.

- [37] Z. Jin *et al.*, "EEG classification using sparse Bayesian extreme learning machine for brain–computer interface," *Neural Comput. Appl.*, to be published. doi: [10.1007/s00521-018-3735-3](https://doi.org/10.1007/s00521-018-3735-3).
- [38] G. Zhou *et al.*, "Linked component analysis from matrices to high-order tensors: Applications to biomedical data," *Proc. IEEE*, vol. 104, no. 2, pp. 310–331, Feb. 2016.
- [39] R. Lai, Y. Mo, Z. Liu, and J. Guan, "Local and nonlocal steering kernel weighted total variation model for image denoising," *Symmetry*, vol. 11, no. 3, p. 329, 2019.
- [40] M. Sandler, A. Howard, M. Zhu, A. Zhmoginov, and L.-C. Chen, "MobileNetV2: Inverted residuals and linear bottlenecks," in *Proc. IEEE Conf. Comput. Vis. Pattern Recognit.*, Salt Lake City, UT, USA, Jun. 2018, pp. 4510–4520.
- [41] W.-Q. Lim, "The discrete shearlet transform: A new directional transform and compactly supported shearlet frames," *IEEE Trans. Image Process.*, vol. 19, no. 5, pp. 1166–1180, May 2010.



JUNTAO GUAN received the B.S. degree in integrated circuit design and integration system from the Harbin University of Science and Technology, in 2016. He is currently pursuing the Ph.D. degree in electronics science and technology with Xidian University, China.

His research interests include image process, computer vision, and deep learning.



RUI LAI received the B.S. degree in information engineering from Xidian University, in 2002, and the M.S. and Ph.D. degrees in electronic science and technology, in 2005 and 2007, respectively.

From 2009 to 2010, he was the Postdoctoral Researcher with the Optoelectronic Science and Engineering Department, Huazhong University of Science and Technology. Since 2010, he has been an Associate Professor with the Microelectronics Department, Xidian University. He has authored more than 60 journal and conference papers. His research interests include computational photography, image sensors, image processing, and deep learning.



AI XIONG received the B.S. and M.S. degrees in automation and control theory and engineering from Chongqing University, Chongqing, in 2002 and 2005, respectively, and the Ph.D. degree in signal and information processing from the Institute of Optics and Electronics, Chinese Academy of Sciences, Chengdu, China, in 2008.

From 2008 to 2016, he was a Research Assistant with the Institute of Optics and Electronics, Chinese Academy of Sciences. Since 2016, he has been an Associate Professor with the Control engineering College, Chengdu University of Information Technology, Chengdu. His research interests include optical sensors, high precision servo control, and adaptive control.

• • •